AD-A098 532 ARMY ELECTRONICS RESEARCH AND DEVELOPMENT COMMAND FO--ETC F/6 20/12
ANALYSIS OF ELECTRICALLY ACTIVE IMPURITY LEVELS IN IN-SITU COMP--ETC(U)
MAR 81 H A LEUPOLD, J J WINTER, R L ROSS

UNCLASSIFIED DELET-TR-81-7 NL

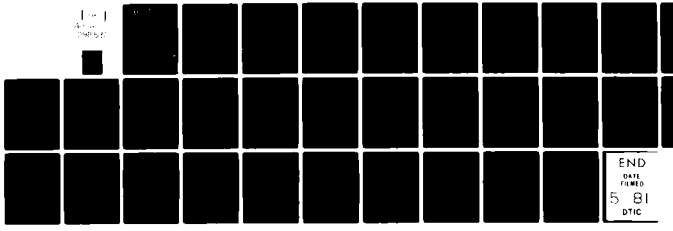

END
DATE FILMED
5 81
DTIC

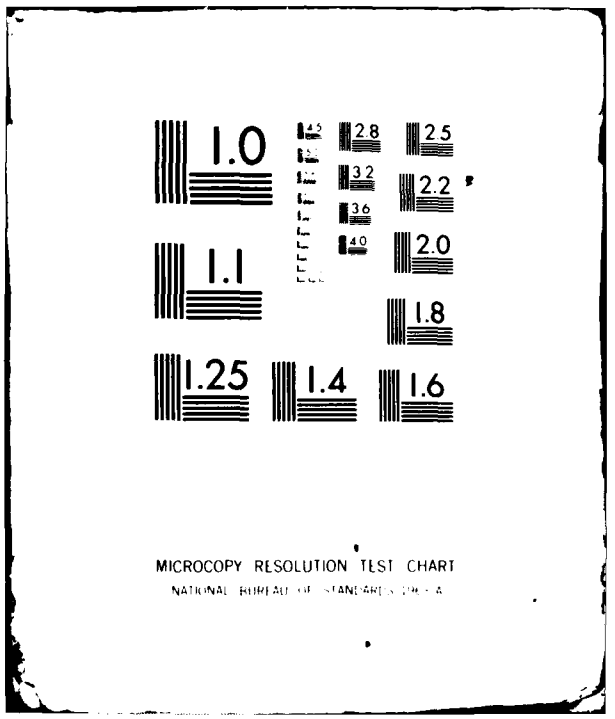
1.0
1.1
1.25
1.4
1.6
1.8
2.0
2.2
2.5
2.8
3.2
3.6
4.0
MICROCOPY RESOLUTION TEST CHART
NATIONAL BUREAU OF STANDARDS 1963-A

LEVEL II

RESEARCH AND DEVELOPMENT TECHNICAL REPORT

DELET-TR-81-7

AD A098532

ANALYSIS OF ELECTRICALLY ACTIVE IMPURITY LEVELS IN IN-SITU COMPOUNDED SEMI-INSULATING GALLIUM ARSENIDE

H. A. LEUPOLD
J. J. WINTER
R. L. ROSS
T. R. AUCOIN

ELECTRONICS TECHNOLOGY & DEVICES LABORATORY

MARCH 1981

ERADCOM

US ARMY ELECTRONICS RESEARCH & DEVELOPMENT COMMAND
FORT MONMOUTH, NEW JERSEY 07703

NOTICES

Disclaimers

The citation of trade names and names of manufacturers in this report is not to be construed as official Government indorsement or approval of commercial products or services referenced herein.

Disposition

Destroy this report when it is no longer needed. Do not return it to the originator.

UNCLASSIFIED

SECURITY CLASSIFICATION OF THIS PAGE (When Data Entered)

(14) DELET-TR-81-7

REPORT DOCUMENTATION PAGE

READ INSTRUCTIONS BEFORE COMPLETING FORM

1. REPORT NUMBER: DELET-TR-81-7	2. GOVT ACCESSION NO.: AD-A098532
3. RECIPIENT'S CATALOG NUMBER:	
4. TITLE (and Subtitle): (6) ANALYSIS OF ELECTRICALLY ACTIVE IMPURITY LEVELS IN IN-SITU COMPOUNDED SEMI-INSULATING GALLIUM ARSENIDE	5. TYPE OF REPORT & PERIOD COVERED:
	6. PERFORMING ORG. REPORT NUMBER:
7. AUTHOR(s): (10) H.A. Leupold, J.J. Winter, R.L. Ross, T.R. AuCoin	8. CONTRACT OR GRANT NUMBER(s): (15)
9. PERFORMING ORGANIZATION NAME AND ADDRESS: Electronic Materials Research Division, US Army Electronics Technology & Devices Laboratory (ERADCOM) Fort Monmouth, NJ 07703 DELET-ES-S	10. PROGRAM ELEMENT, PROJECT, TASK AREA & WORK UNIT NUMBERS: 61102A (10) 1L161102AH47 02 051
11. CONTROLLING OFFICE NAME AND ADDRESS: US Army Electronics Research & Development Command, Fort Monmouth, NJ 07703, DELET-ES-S	12. REPORT DATE: (11) March 1981
	13. NUMBER OF PAGES: 36
14. MONITORING AGENCY NAME & ADDRESS(if different from Controlling Office):	15. SECURITY CLASS. (of this report): (12) 42
	15a. DECLASSIFICATION/DOWNGRADING SCHEDULE:

16. DISTRIBUTION STATEMENT (of this Report)

Approved for public release; distribution unlimited.

17. DISTRIBUTION STATEMENT (of the abstract entered in Block 20, if different from Report)

18. SUPPLEMENTARY NOTES

19. KEY WORDS (Continue on reverse side if necessary and identify by block number)

Gallium Arsenide, Compensation, Mixed Conduction, In-situ Compounding, Semi-insulating

20. ABSTRACT (Continue on reverse side if necessary and identify by block number)

Conductivity and Hall measurements were made on semi-insulating GaAs samples grown with a recently developed process using in-situ compounding with liquid encapsulated (B_2O_3) Czochralski growth techniques. Mixed conduction analysis in combination with a nomographic analysis of charge balance and conduction was used to elucidate compensation in this material. Given the Cr concentration in one sample, the use of an iterative self-consistent procedure allowed the deduction of total donor and acceptor concentrations for identically prepared Cr-doped and undoped

(Cont'd on reverse side)

DD FORM 1 JAN 73 1473 EDITION OF 1 NOV 65 IS OBSOLETE

UNCLASSIFIED

SECURITY CLASSIFICATION OF THIS PAGE (When Data Entered)

samples. Further analysis yielded the compensation ratio and energy level of the dominant acceptor of a third specimen. A subsequent spark source analysis confirmed the high purity of this in-situ compounded material, as well as the conclusions and utility of the nomographic analysis.

CONTENTS

TABLE

FIGURES

INTRODUCTION

The current extension of the operating spectrum of military devices to ever higher frequencies has given rise to a greatly increased need for reproducible and reliable GaAs material and devices. Effective fulfillment of this need requires an in-depth understanding of the quantities actually being measured by the various characterization experiments and how they relate to actual device performance. Such an understanding is presently lacking in many instances, and its acquisition necessitates a more methodical approach for the marshalling of the various characterization data into a clear, coherent picture of the underlying compositions and processes.

In particular, the ongoing efforts in this laboratory to produce high-purity semi-insulating GaAs (1) require just such an approach to provide, on a rapid and interactive basis, useful information on the carrier type, concentration and mobility from resistivity and Hall measurements, as well as a guide to modeling and altering the microscopic material properties via manipulation of impurity content, heat treatment, etc.

These ends have been achieved with a procedure which combines mixed conduction analysis (2,3) with a nomographic method based on ideas employed by Shockley and others (4,5) to determine Fermi levels from known impurity concentrations, and more recently by Zucca (6) to qualitatively display the relative merits of two competing models of compensation in GaAs. In this report we analyze the results of several measurements to develop a tentative model of the electrically active impurity structure of material developed in this laboratory.

EXPERIMENTAL

A silicon and carbon-free modification of the liquid encapsulated Czochralski technique (1) employing in situ compounding was used to grow the samples measured. Van der Pauw measurements of conductivity and Hall coefficient were made at various magnetic fields up to a value of 19 kOe. The apparatus, shown in Figure 1a, is a fully guarded system capable of measuring resistances of over 10^{12} ohms (7). It has been automated as shown in Figure 1b. Semi-insulated GaAs presents special contacting and measurement problems. Initially we used soldered indium contacts, but later changed to tin contacts alloyed in a Penzac furnace at 400C for 5 minutes in flowing hydrogen. This method proved more reliable in achieving ohmic response.

NOMOGRAPHIC ANALYSIS

The method evolves from a consideration of the expression for the Fermi occupation probability of a level of energy E and degeneracy g. In a system with Fermi energy E_f at an absolute temperature T this expression is

$$f = (1 + g \exp\{(E - E_f)/kT\})^{-1} \qquad (1)$$

Usually the occupation probabilities of the different energy levels are plotted for a particular value of the Fermi energy E_f, and the familiar curve of Figure 2a results. For the present purpose we consider instead the

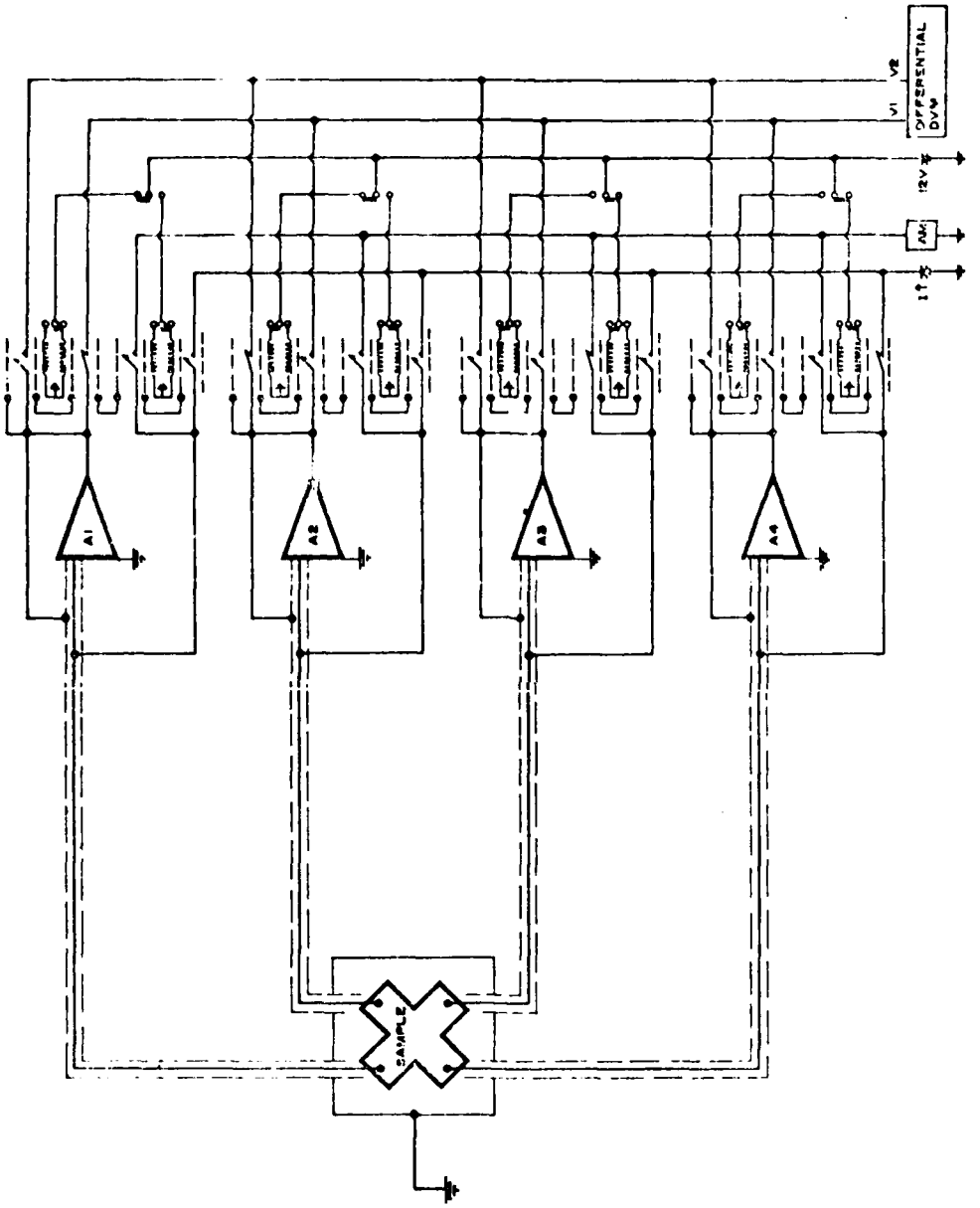

Figure 1a. Guarded Van der Pauw system.

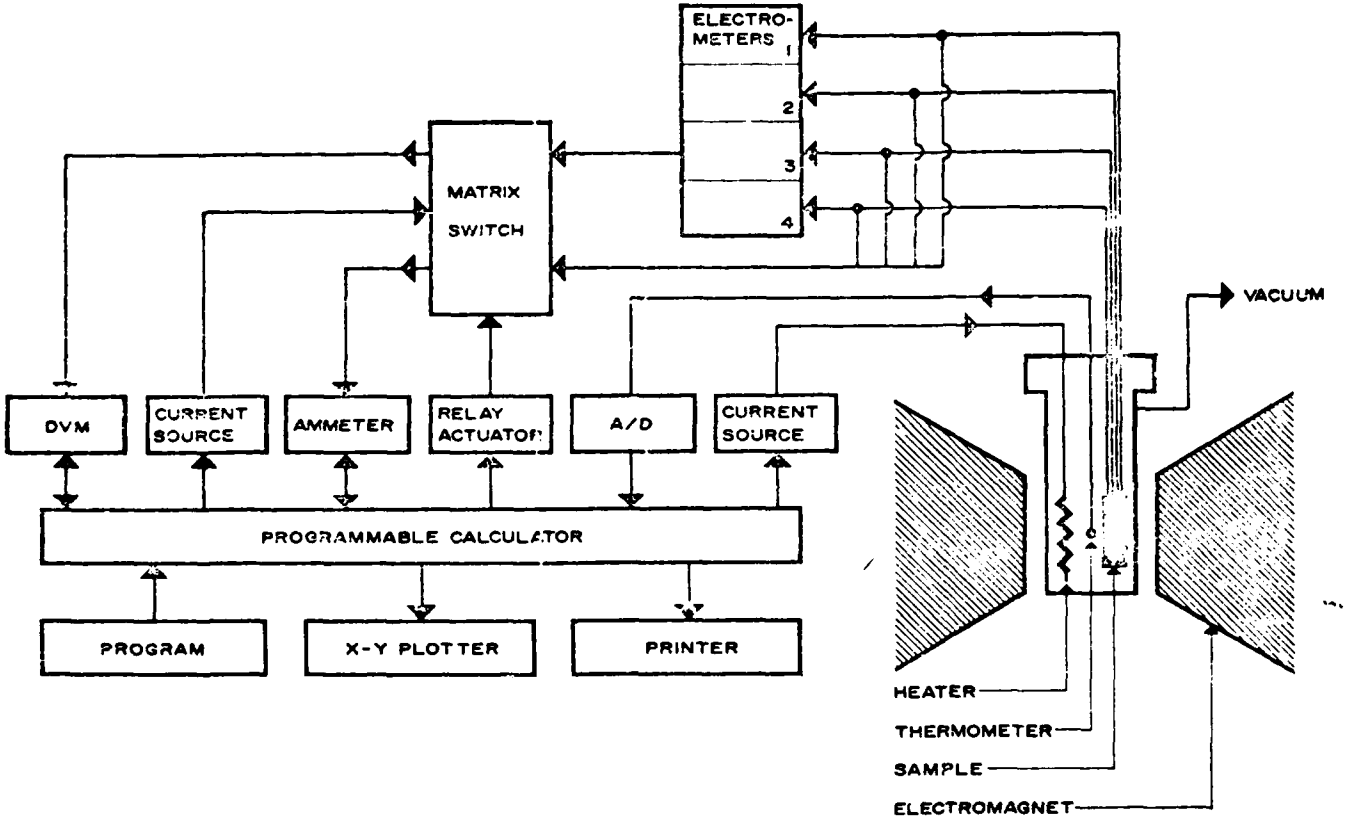

Figure 1b. Automated Van der Pauw Hall and resistivity measurement system. The sample is contained in a fully shielded, evacuated chamber and is connected to four (Keithley 602) electrometers by triaxial cable, the inner shield of which is driven by the output of each electrometer. Shielded coaxial reed relays provide the required lead switching capability.

occupation probability of a particular energy level E_i as a function of the Fermi energy, and we then obtain the curve in Figure 2b. The step in this curve occurs in the neighborhood of $E_f=E_i$ and is of approximately exponential form. If it is drawn on a semi-log scale, the exponential appears as a straight line (as in Figure 2c), the slope of which is given by 1/kT. Hereafter, base 10 logarithms will be used and, accordingly, slopes will be given by (log e)/kT. A similar curve can also be drawn for a particular hole level, but in that case the slope of the occupancy curve is reversed in sign. In an intrinsic semiconductor the only energy levels which play a role in conductivity are the electron levels in the conduction band and the hole levels in the valence band. If one sums the contributions of all these levels, assuming the usual (5) free electron parabolic dependence, and g in Equation (1) is taken to be 1, the solid curves of Figure 3a result. If one replaces the parabolic distribution with equivalent single levels of multiplicity N_c and N_v, the dashed curves in Figure 3a result and merge with solid curves in the region of interest inside the gap. This is because only the N_c or N_v states that lie within increments of kT from the edges of their respective gaps contribute significantly to the portions of the curves lying within the gap. Usually intrinsic semiconductors are characterized by N_c and N_v, the effective "densities of states" for the conduction and valence bands (4.7×10^{17} and 7.0×10^{18} cm^{-3} respectively) and the band gap at 295k, $E_c-E_v=1.42$ eV (8) Figure 3a represents intrinsic GaAs at room temperature. The levels E_c and E_v of the n and p curves define the band gap. Since the occupancy numbers are simply the concentrations of carriers n, p in the conduction and valence bands respectively, charge conservation demands that n = p. For this condition to be fulfilled the Fermi energy of the system must be that at the intersection of the curves for n and p, and the values of the latter at this point (n_s and p_s respectively) are the electron and hole concentrations that actually prevail. Since this material is intrinsic, n_s is equal to n_i and has a value of $1.6 \times 10^6/cm^3$. Figure 3b shows the effect of raising the temperature from T_1 to T_2 on intrinsic material like GaAs, where N_v is greater than N_c. The intersection of the n and p curves moves to a higher value of E_{fs} and n_s.

The forthcoming discussions will show that the analytic power and versatility of the nomographs can be considerably enhanced by the introduction of a conductivity vs Fermi energy curve. This is usually accomplished by inserting the values of the mobilities μ_n and μ_p, derived from mixed conduction analysis of conductivity and Hall data, into the expression for conductivity.

$$\sigma = e \{\mu_n n(E_f) + \mu_p p(E_f)\} \qquad (2)$$

Figure 3a shows a plot of σ as a function of Fermi energy for an ideal intrinsic sample with lattice-limited mobilities of $\mu_n = 8000$ and $\mu_p = 400$ $cm^2/V\text{-sec}$. It is interesting to note how the high mobility ratio has shifted the conductivity minimum to an energy considerably below the Fermi level, thus rendering minimum conductivity impossible in the absence of impurities. Indeed, the shift is just sufficient to take the sample beyond the edge of the mixed conduction region (i.e., out of the rounded portion of the curve) so that the measured Hall mobility for such a sample would, for all practical purposes, be identical to the true electron mobility μ_n.

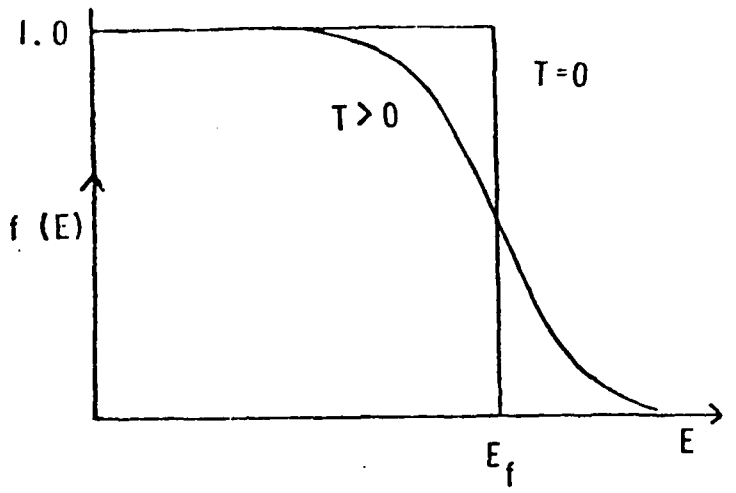

Figure 2a. Plot of level occupation probability $f = (1+\exp (E-E_f)/kT)^{-1}$ as a function of energy, E, for a particular Fermi energy E_f.

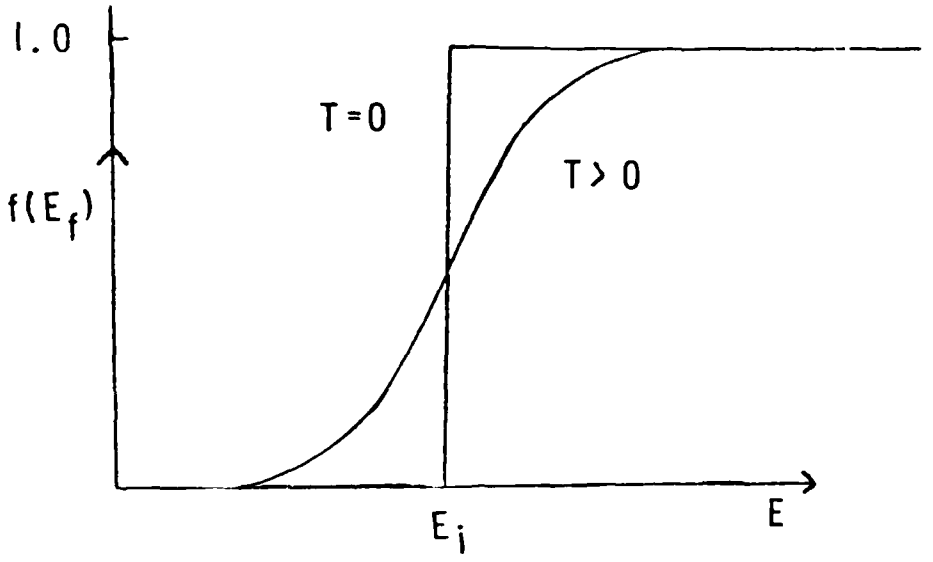

Figure 2b. Plot of occupation probability for an energy level E_i as a function of Fermi energy Ef.

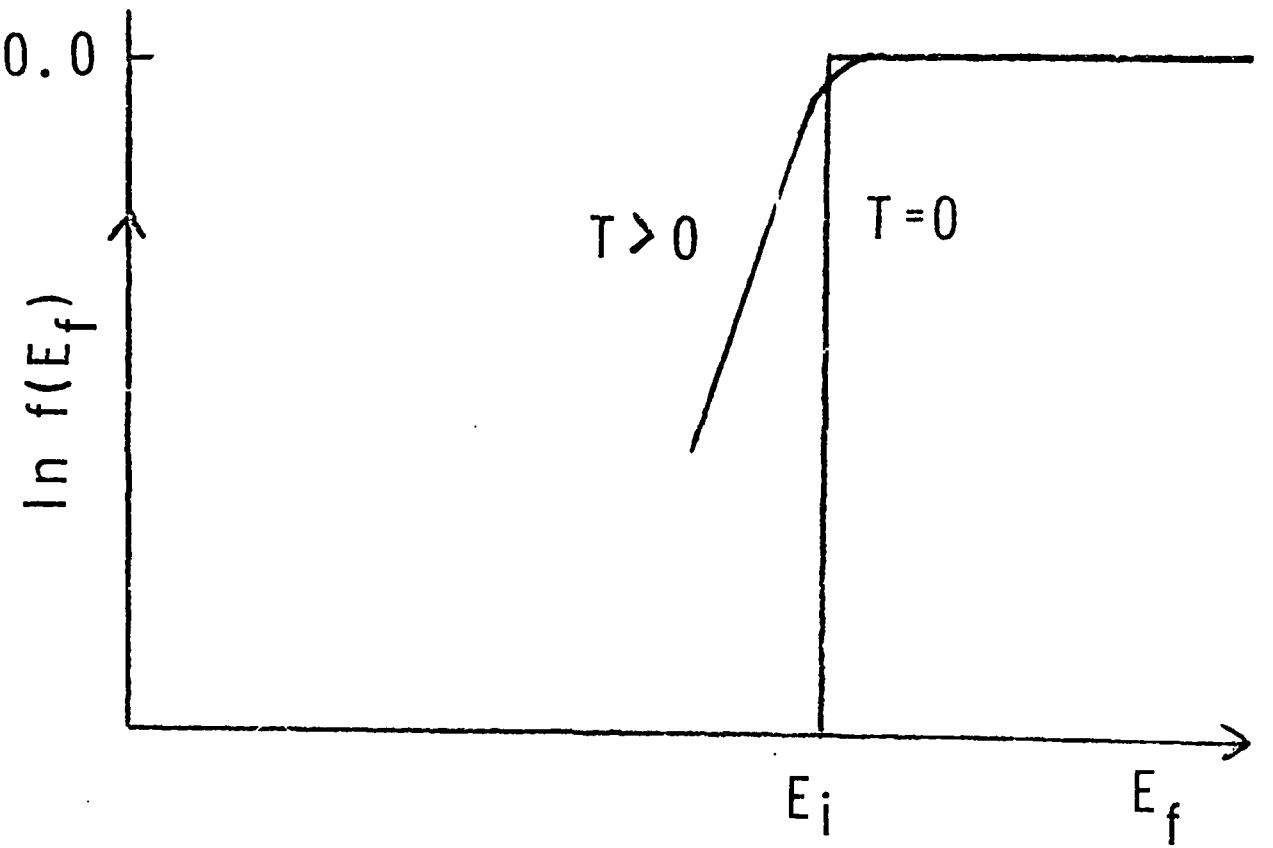

Figure 2c. Semi-log plot of occupation probability of level E_i as a function of E_f.

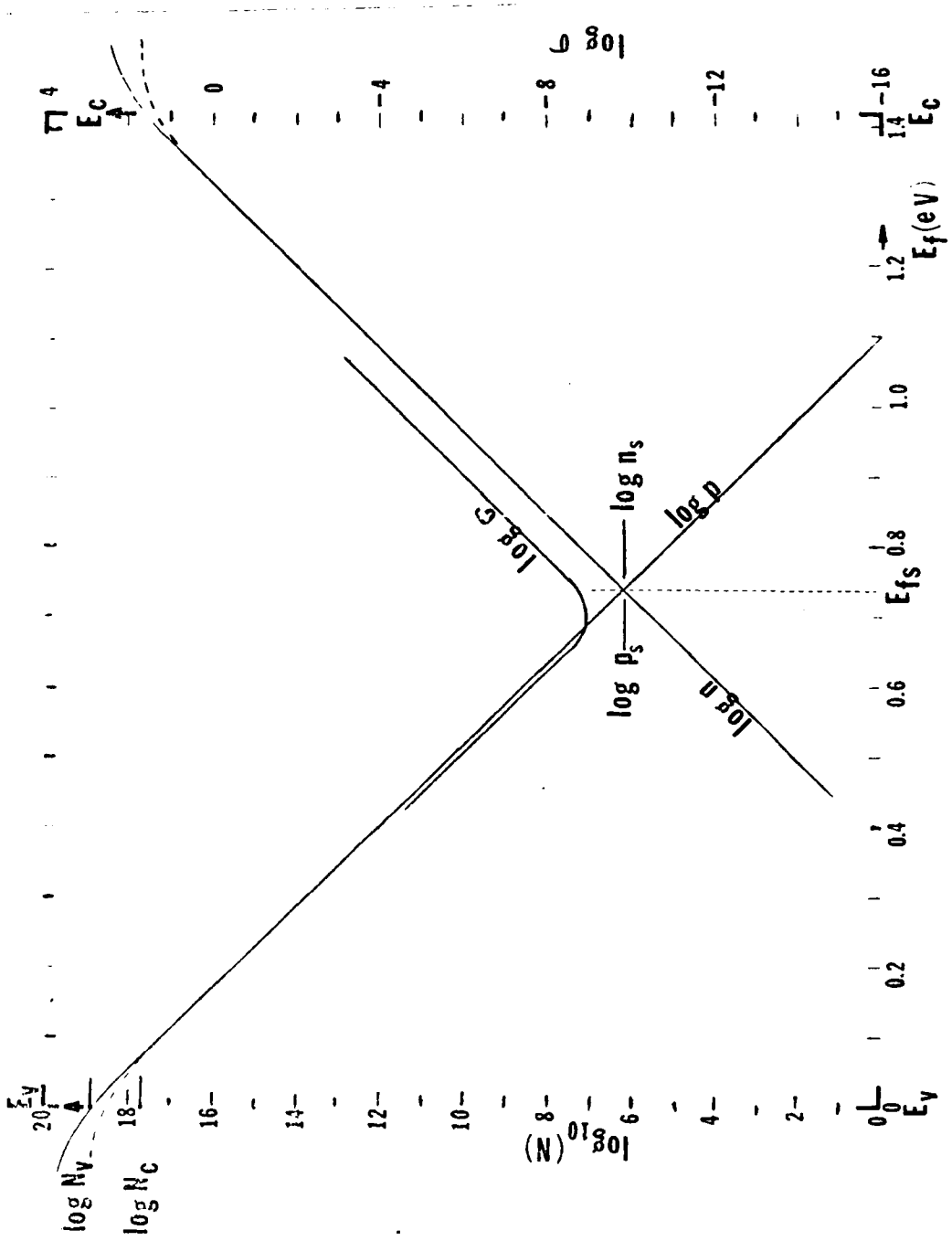

Figure 3a. Charge balance plots for intrinsic GaAs. N represents both functions n and p. The intersection point of these curves determines the actual or system carrier concentration n_s and p_s as well as the Fermi level of the system E_{fs}. Since this material is intrinsic $n_s = n_i = p_s$ as shown. Conductivity, σ, is also plotted for electron and hole mobilities of 8000 and 400 cm^2/V-sec respectively.

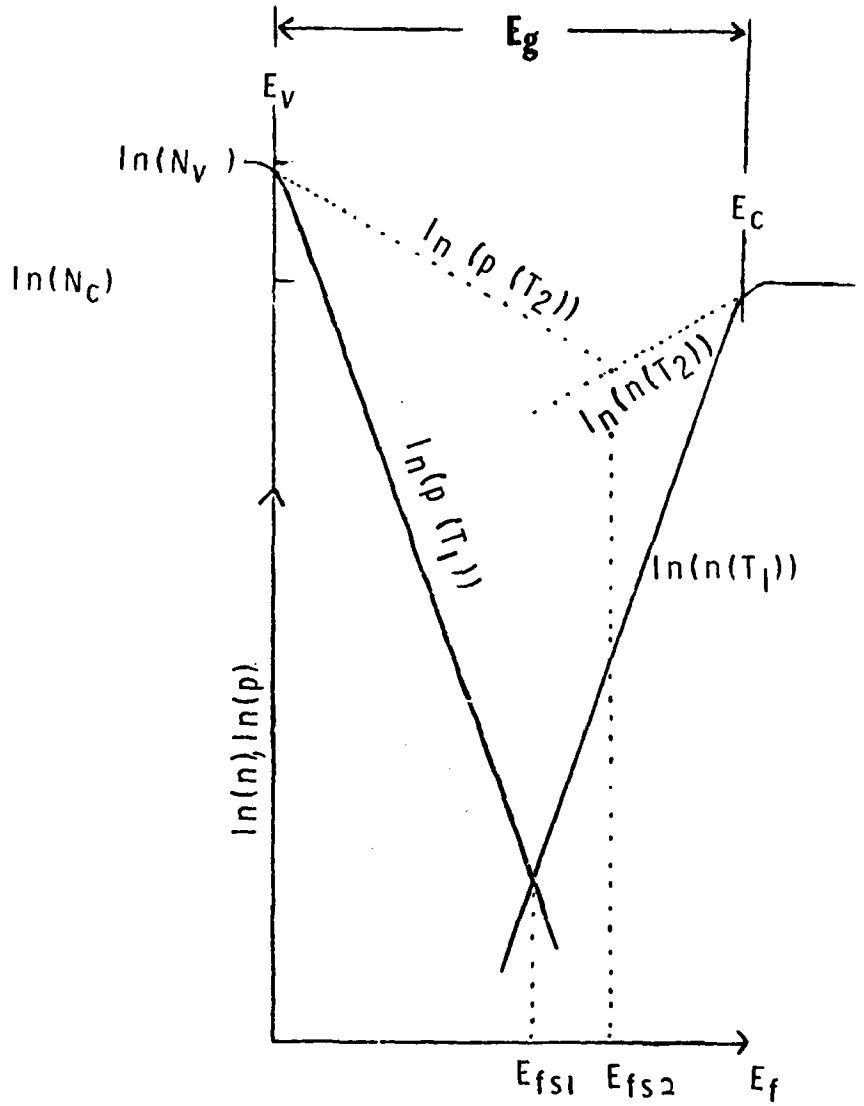

Figure 3b. The effect of temperature on the Fermi level E_{fs}, the electron, n, and hole, p, densities.

If impurity donors and acceptors are present, the charge conservation condition becomes

$$n + \sum_a N_a^- = p + \sum_d N_d^+, \qquad (3)$$

where N_a^- and N_d^+ are the numbers of ionized acceptor and donor levels respectively, and are given by the Fermi occupation probability multiplied by their respective concentrations, i.e.:

$$(N_a^- , N_d^+) = \frac{(N_a, N_d)}{1 + g \exp\left(\{(E_a, -E_d) \mp E_f\}/kT\right)} \qquad (4)$$

where g is taken to be 2 for donors and 4 for acceptors*(6). To facilitate graphical construction and analysis, drafting templates were made of the p and n curves, of the curves for Equation (4) with g=1,2,4, and for the smooth curves that occur at junctions between any two of the foregoing.

Figure 3c illustrates the case where a single deep donor is present. Here the charge conservation condition for this hypothetical sample is simply

$$n = p + N_d^+$$

and

$$\log n = \log (p + N_d^+)$$

Note how over most of the range of the plot for the right side of this equation either p or N_d^+ dominates and the curve for the sum is either

$$\log (p + N_d^+) \approx \log p$$

or

$$\log (p + N_d^+) \approx \log N_d^+$$

The dashed lines indicate how each of the constituent curves would continue in the absence of the others. Thus, it is very easy to form the sum curve for $\log (p+N_d^+)$ from its constituents, since it is identical to that of the dominant constituent except in the neighborhood of the point where the

*The values of g for deep donors and acceptors are really not known. The frequently (6) used values are 1 for each, or 2 and 4 respectively. Since, as will be shown, either choice could be made with little effect on the accuracy of the results, the values of 2 and 4 are maintained throughout the paper.

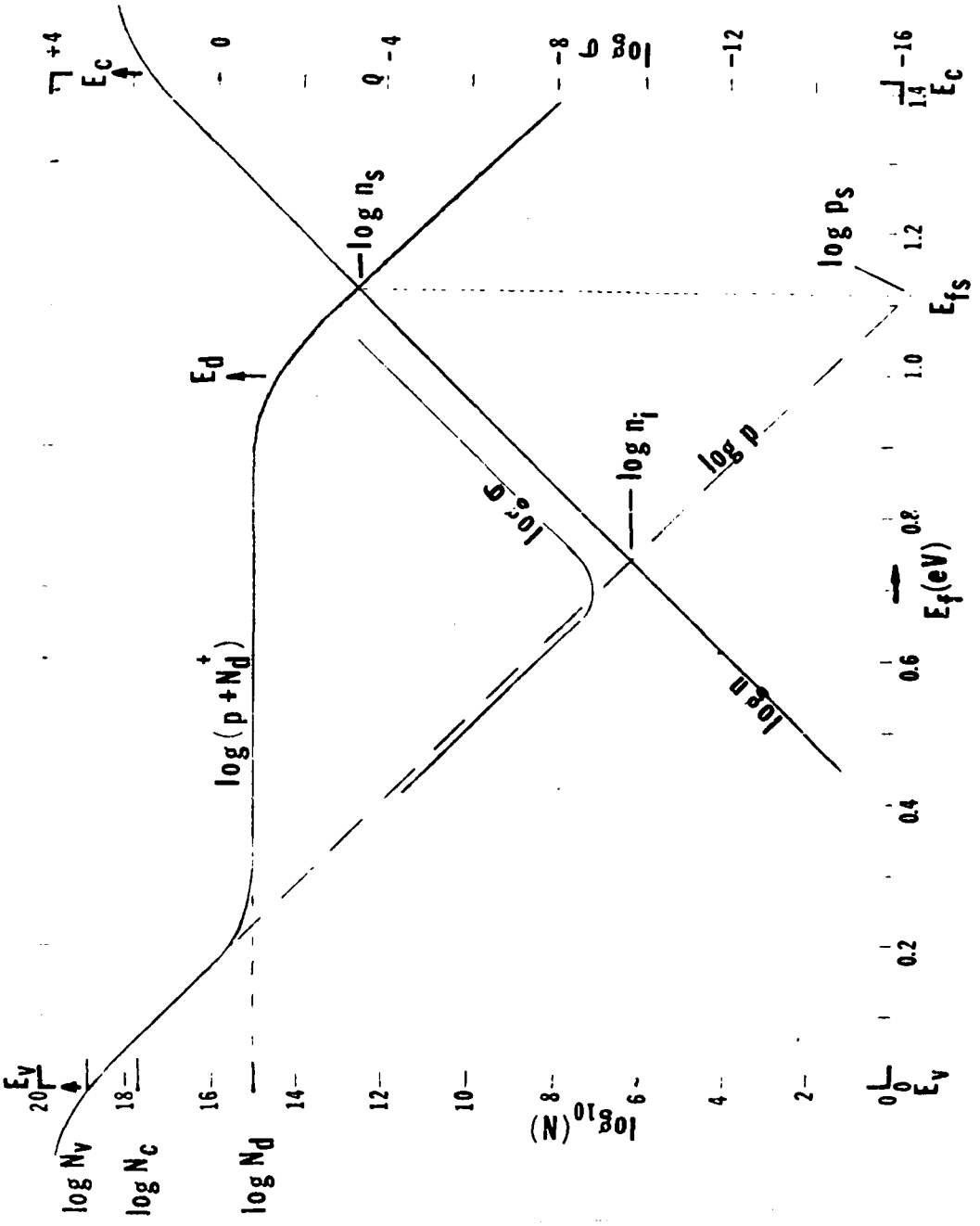

Figure 3c. Charge balance plot for a system having a single donor N_d of energy level E_d and no acceptors. N represents each of the functions, n, p and $(p+N_d^+)$. The dashed lines indicate how each of the constituent curves would continue in the absence of the other. Note charge balance is achieved at the intersection of the two solid curves. Projecting this point onto the n and p curves along the Fermi level axis determines the system Fermi level E_{fs}, and the system values of the n and p concentrations n_s and p_s, respectively. Conductivity, σ, is also plotted for electron and hole mobilities of 7000 and 350 cm^2/V-sec respectively.

constituents join. Here a numerical plot of the sum yields a smooth continuous "joint" between the dominant constituent curves as shown. Notice that in the charge balance equation and its graphical representation, the valence band behaves as a donor and the conduction band as an acceptor. This is clear when we consider that both members of the former category furnish electrons with the donor assuming a positive charge, while the two latter species accept electrons with the acceptor assuming a negative charge. Once again the intersection of solid or sum curves determines the system Fermi level, E_{fs}, and electron and hole concentrations n_s and p_s. Here n_i is defined, as usual, by the intersection of what would be the intrinsic electron and hole curves. The plausible values of μ_n= 7000 and μ_p= 350 cm^2/V-sec used to construct the conductivity curve were chosen from an empirical graph (9) which relates the mobilities to impurity concentration.

Thus, via the foregoing we can analyze the electrical properties of any material. One proceeds with the formation of plus and minus curves by respective summations of ionized donor curves with the p curve, and ionized acceptor curves with the n curve. The Fermi level is then determined by the intersection of the plus and minus curves. The electron and hole concentrations are subsequently obtained from the intrinsic n and p curves at the Fermi level thus determined. These, together with a knowledge of the mobilities, yield the conductivity and Hall coefficient. The process can also be applied in the inverse manner, i.e., from a mixed conduction analysis of Hall and conductivity data one can determine n, and then, using the nomograph, determine E_{fs} and the relative concentration of the assumed electrically active impurities. These concentrations can then sometimes be used in conjunction with the same analysis of related material to deduce the nature and concentrations of other electrically active impurities, as is done below.

MIXED CONDUCTION ANALYSIS

In well compensated materials dominated by mid-gap impurities, conductivity approaches a minimum and conduction of both carrier types becomes comparable; thus necessitating mixed conduction analysis. As Putley (10) observes, the total or measured Hall coefficient R, and conductivity σ, vary with magnetic field B, as

$$R = \frac{R_n \sigma_n^2 + R_p \sigma_p^2 + R_n R_p \sigma_n^2 \sigma_p^2 (R_n + R_p) B^2}{(\sigma_n + \sigma_p)^2 + \sigma_n^2 \sigma_p^2 (R_n + R_p)^2 B^2} \qquad (5)$$

$$\sigma = \frac{(\sigma_n + \sigma_p)^2 + \sigma_n^2 \sigma_p^2 (R_n + R_p)^2 B^2}{\sigma_n (1 + R_p^2 \sigma_p^2 B^2) + \sigma_p (1 + R_n^2 \sigma_n^2 B^2)} \qquad (6)$$

where n and p refer to the electrons and holes respectively.

Taking $R=0$, $R_n = -1/ne$, $\sigma_n = n\mu_n e$, $R_p = 1/pe$ and $\sigma_p = p\mu_p e$

$$R = \frac{-ne\mu_n^2 + pe\mu_p^2}{(pe\mu_p + ne\mu_n)^2} = \frac{-n + p\,(\mu_p/\mu_n)^2}{e[n + p(\mu_p/\mu_n)]^2}$$

$$\sigma = \sigma_n + \sigma_p = ne\mu_n + pe\mu_p + [n + p\,(\mu_p/\mu_n)]\mu_n e$$

$$\mu_H = R\sigma = \mu_n \frac{(-n + p\,(\mu_p/\mu_n)^2)}{n + p\,(\mu_p/\mu_n)} = \mu_n \frac{(-n + p\,(b)^2)}{n + p\,(b)} \qquad (7)$$

From this equation we can observe how closely the Hall mobility μ_H, tracks the electron mibility μ_n as a function of electron and hole concentrations, n and p, and mobility ratio, μ_p/μ_n or b.

Since $R = \dfrac{-\sigma_n\mu_n + \sigma_p\mu_p}{\sigma^2}$

R can be negative even when σ_p is greater than σ_n, that is when the holes are the dominant carrier. Since a ratio, b^{-1}, or μ_n/μ_p of 15 to 20 is, as we shall see, not at all unreasonable in GaAs, the materials could in fact exhibit appreciable p type behavior along with a negative Hall coefficient.

We rewrite μ_H as $\mu_H = R\sigma = \dfrac{-\sigma_n\mu_n + \sigma_p\mu_p}{\sigma_n + \sigma_p}$ so we can consider it at minimum conductivity where $\sigma_p = \sigma_n$, as we can see from Figure 3. Therefore

$$\mu_H(\sigma\ \text{min}) = -\frac{\mu_n + \mu_p}{2} = \frac{\mu_n(1-b)}{2} \qquad (8)$$

Thus, for small values of b, μ_H is about half μ_n at minimum conductivity. The Hall mobility approaches μ_n as the conductivity (see Figure 3) becomes linear with increasing Fermi energy and n becomes greater than p, as is also implied by Equation (7) for small b. In any case, outside the rounded region of the conductivity curve the Hall mobility measurement gives the electron mobility for $n \gg p$ and the hole mobility for $p \gg n$. Table I shows μ_p and μ_H for representative values of b and μ_n.

In general, to determine the carrier concentrations and mobilities in the rounded conductivity or mixed conduction region we require other measurements or equations to those listed above. Look developed an analysis (2, 11) of Equations (5) and (6) which assumed that single carrier magnetic field dependencies were not significant. Recent data (12) indicates that such effects are important, and Look* (3) has developed a new analysis which employs a simi-empirical relationship between μ_n and μ_p and a tentative value of n_i to generate a family of curves relating μ_n to μ_H through the resistivity ρ (see Figure 4). For $\rho_o < 4 \times 10^8$ Ω-cm, $\mu_n = \mu_H$, in agreement with our graphical analysis for typical values of μ_n. For $\rho_o > 4 \times 10^8$ the curves become double valued, with one of the values always equal to μ_H, and additional information such as that provided by the dependence of ρ and R on field is required for unique determination of μ_n.

Look argues that it should be possible to relate μ_p to μ_n in principle, since the carrier scattering mechanisms are similar. He tentatively proposed

$$\mu_p^{-1} = 9 \times 10^{-4} + 13\mu_n^{-1} \qquad (9)$$

As Table 1 shows, this implies b^{-1} varies from 14 to 20 for $1000 < \mu_n < 8000$. A least squares plot (9) of μ_H against impurity concentrations, as estimated by $(Re)^{-1}$, in conducting samples dominated by shallow impurities implied the relationship $\mu_p = \mu_n/19$ over most of the range. See data listed under Reference (9) of Table 1. The n and p mobilities ranged from 7×10^3 to 3.6×10^3, and about 360 to 196 cm^2/Volt sec respectively over a concentration range of $10^{15} - 4 \times 10^{17}$ cm^{-3}. In contrast, the p and n mobilities in germanium and silicon, respectively, diverged and converged considerably with increasing impurity concentration. There is scattering in the GaAs plot (90% of the points are within 15% of the line), and its application to samples dominated by deep impurity levels is questionable; but it does tend to confirm that a slowly varying statistical relationship between mobilities may exist in GaAs, and it provides some confirmation of the amplitude of the mobility ratio.

Table 1 summarizes much of the foregoing. Therein values of μ_p deduced from μ_n using Equation (9) are shown. We use these values in Equation (8) which represents μ_H at σ_{min}, where $\sigma_p = \sigma_n$ or $p = n(\mu_n/\mu_p)$, the center of the mixed conduction region. At this point μ_H is about half μ_n for the mobility ratios, μ_n/μ_p considered. As n approaches and slightly exceeds p, μ_H approaches μ_n and the Fermi level approaches the edge of the rounded mixed conduction region. See Figure 3 and Equation (7).

* Look examined the solutions of some 55 Cr doped and 17 O doped (or undoped) semi-insulating GaAs crystals using different forms of $\mu_p = f(\mu_n)$, n_i was allowed to range from (1-15) $\times 10^6$ cm^{-3} and μ_n from (1-8) $\times 10^3$ cm^2/V-sec. Nine samples had no solutions for $n_i < 4 \times 10^6$ cm^{-3}, seven had no solutions for $n_i < 1.5 \times 10^6$ cm^{-3}. The value of n_i having the fewest "violations" was $n_i = 2.6 \times 10^6$ (cm^{-3}) and it was tentatively chosen for his calculations.

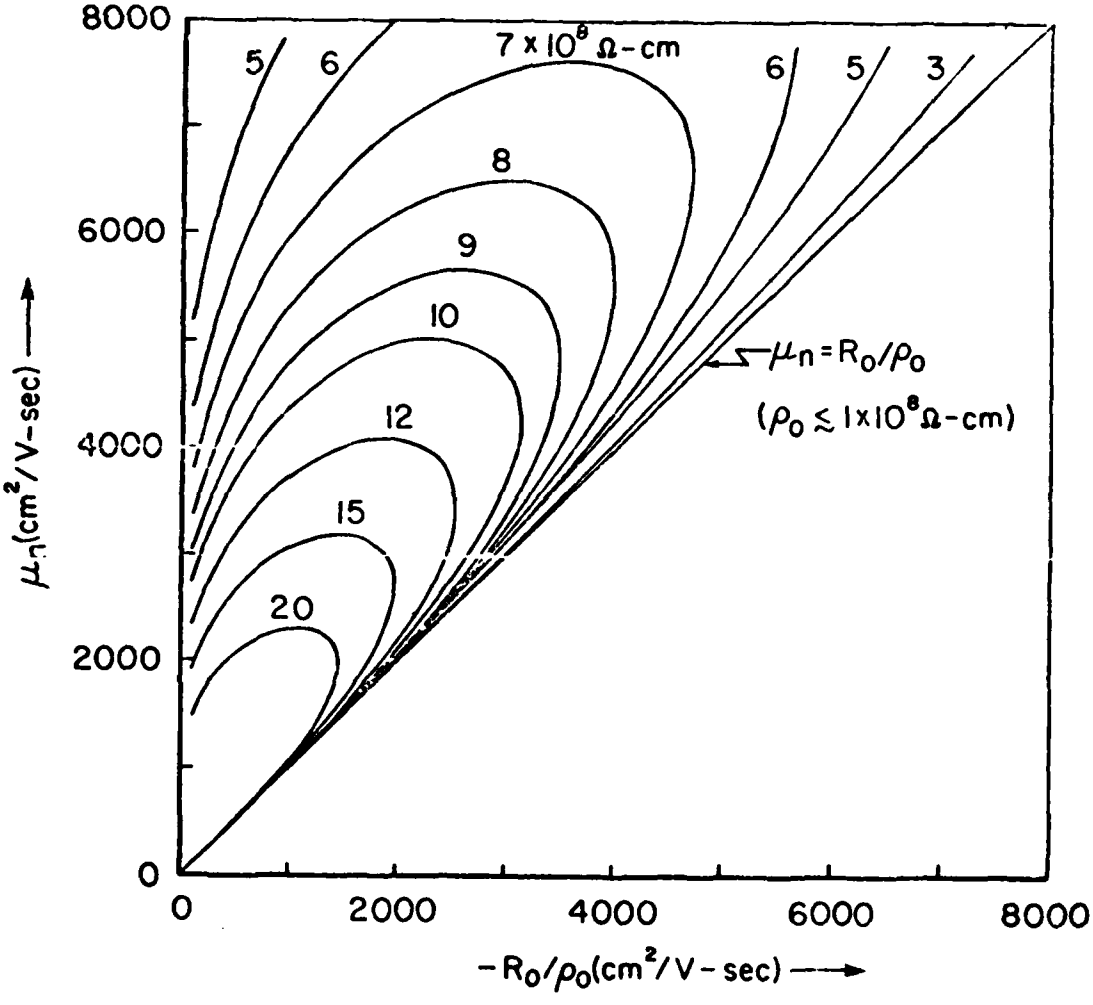

Figure 4. Plots of μ_n Vs R_0/ρ_0 for various values of ρ (units of 10^8 Ω-cm) for samples with negative (n-type Hall coefficient).

The analysis applied here showed that for each of the samples studied conduction was outside the mixed conduction region; therefore, μ_H was the appropriate value of μ_n. Thus the results were insensitive to the exact choice of parameters tentatively proposed by Look and used to deduce the alternate or mixed conduction value of μ_n.

TABLE

Calculated values of hole, μ_p and Hall, μ_H, mobility as a function of electron mobility, μ_n for $p = n$ and $p = (b^{-1})\,n$ where (b^{-1}) is the mobility ratio (μ_n/μ_p). As explained in the text, $p = (b^{-1})n$ occurs at the center of the mixed conduction region, where $\mu_H = (\mu_n/2)\,(1-b)$, and for high values of b^{-1}, $p = n$ occurs just inside the edge of the mixed conduction region as indicated by the values of μ_H/μ_n shown. Equation 9 by Look (3) relating μ_p to μ_n was used in the calculation of μ_H. Values of μ_p and b^{-1} from a least squares plot by Sze (9) on single carrier dominated specimens were included to afford some comparison with experimentally obtained values.

μ_p (Ref 9)	b^{-1} (Ref 9)	μ_n	μ_p (Eq 9)	b^{-1} (Eq 9)	$\mu_H(n=pb)$	$\mu_H(p=n)$	$\mu_H(p=n)/\mu_n$
-	-	8000*	400*	20.0	3800	7580	.96
3.6×10^2	19.3	7000	363	19.1	3320	6630	.95
2.2×10^2	18.2	4000	241	16.6	1880	3760	.94
-	-	2000	135	14.8	932	1860	.93
-	-	1000	72	13.9	464	928	.93

*Lattice limited mobility values.

The ideas and procedures outlined above were applied to analyze four semi-insulating GaAs specimens, thereby to construct self-consistent models of the electrically active impurity levels and concentrations. The completeness of the models and the amount of extractable information they provide depend on the amount of prior electrical and chemical information available for each respective sample.

The specimen about which the most a priori knowledge was available was that reported by Lindquist (13), who had analyzed it chemically (spark source mass spectroscopy) and measured its Hall coefficient and resistivity. From this information it proved possible to construct a complete charge-balance diagram to check the various electrical parameters, impurity concentrations and energy levels for self-consistency.

The other three samples were in situ compounded materials grown in this laboratory and labeled #9, #11, and #17. Specimens from the #11 boule exhibited some of the lowest conductivities ($<2.5 \times 10^{-9}$ Siemens/cm) reported in the literature for undoped material. Samples #11 and #17 were similarly grown and handled equally in every way except that #17 was deliberately doped with Cr to a concentration of $10^{16}/cm^3$. From this knowledge, and from self-consistent iterative employment of the charge balance-conductivity nomographs, it was possible to estimate total effective acceptor and donor concentrations in both samples.

Sample #9 differed from samples #11 and #17 in that the Ga used in its fabrication was not as pure as that used for the other samples. For this reason it was not possible to arrive at impurity concentrations via the nomographs; but it was feasible to deduce the donor to acceptor concentration ratio, as well as the presence of iron and/or copper impurity atoms.

Sample L

Figure 5 is a nomographic representation or "portrait" of Lindquist's (13) specimen (L) based on his spark source analysis and electrical measurements. Because there are known values for all of the nomographic parameters, the figure is overspecified and can be completely consistent only if all of the values are exactly correct. Since there has been some discussion (14) of the identity and the room temperature value of the energy level of the deep donor DD in GaAs, often identified with oxygen, we will demonstrate the analysis by considering these issues. First, the energy level of oxygen will be considered an unknown and we will allow it to be determined as a function of the other parameters. The procedure is as follows. First a conductivity vs E_f curve is constructed. Mobilities μ_n and μ_p are found by mixed conduction analysis, and the two values of μ_n thus obtained are 879 and 2650 $cm^2/Vsec$. The former is the Hall mobility, and is chosen as the correct value since the latter would result in too low a value of the oxygen impurity energy level as discussed below. The conductivity curve that results from this choice has the measured conductivity σ_A on its linear portion (outside of the mixed conduction region) as it must when $\mu_n = \mu_H$. Thus the conductivity curve reveals the interesting fact that it is possible for a specimen of GaAs to exhibit single carrier dominance while showing a very low conductivity (5.6×10^{-10} Siemens/cm), generally considered characteristic of mixed conduction. The charge balance curves are then drawn as described in the previous section, with the use of the concentration data from the chemical analysis and the energy levels of all of the impurities except that of oxygen, which is to be determined. A gap is left in the (+) curve between E_f = 0.68 and 0.85 eV, which reflects the range in room temperature energy levels associated with oxygen in recent years, (see References(13) and (3) respectively) and which for demonstration purposes is considered here to be the range of uncertainty in the oxygen level. The measured conductivity is then located on the positive slope of the conductivity curve at point A. The positive sense is chosen because the material was determined to be n type from Hall measurements. The energy corresponding to this point is that of the Fermi level of the material. It is therefore clear that the (-) curve must be intersected by the (+) curve at point B in Figure 5. The gap in the (+) curve can then be closed by placing the g = 2 template for oxygen (chosen as explained above) so that its slope passes through B and its plateau coincides with that for the total donor concentration. The oxygen step is then drawn as shown by the dotted portion of the (+) curve in Figure 5. The lower part of the oxygen slope is then joined smoothly to the level representing the sum of all the other donor concentrations. The room temperature energy level thus implied is found to be at 0.76 eV, which is exactly in the center of the range considered. The lower extreme is ruled out because if a donor level existed at 0.68 eV, minimum conductivities would be routinely observed in the absence of Cr. This can be readily seen from a glance at the nomograph. Support for the upper extreme includes a helium temperature value of 0.87 or 0.65 eV below the conduction band (15). However, the upper value cannot be used to explain the low conductivities we and others obtain from

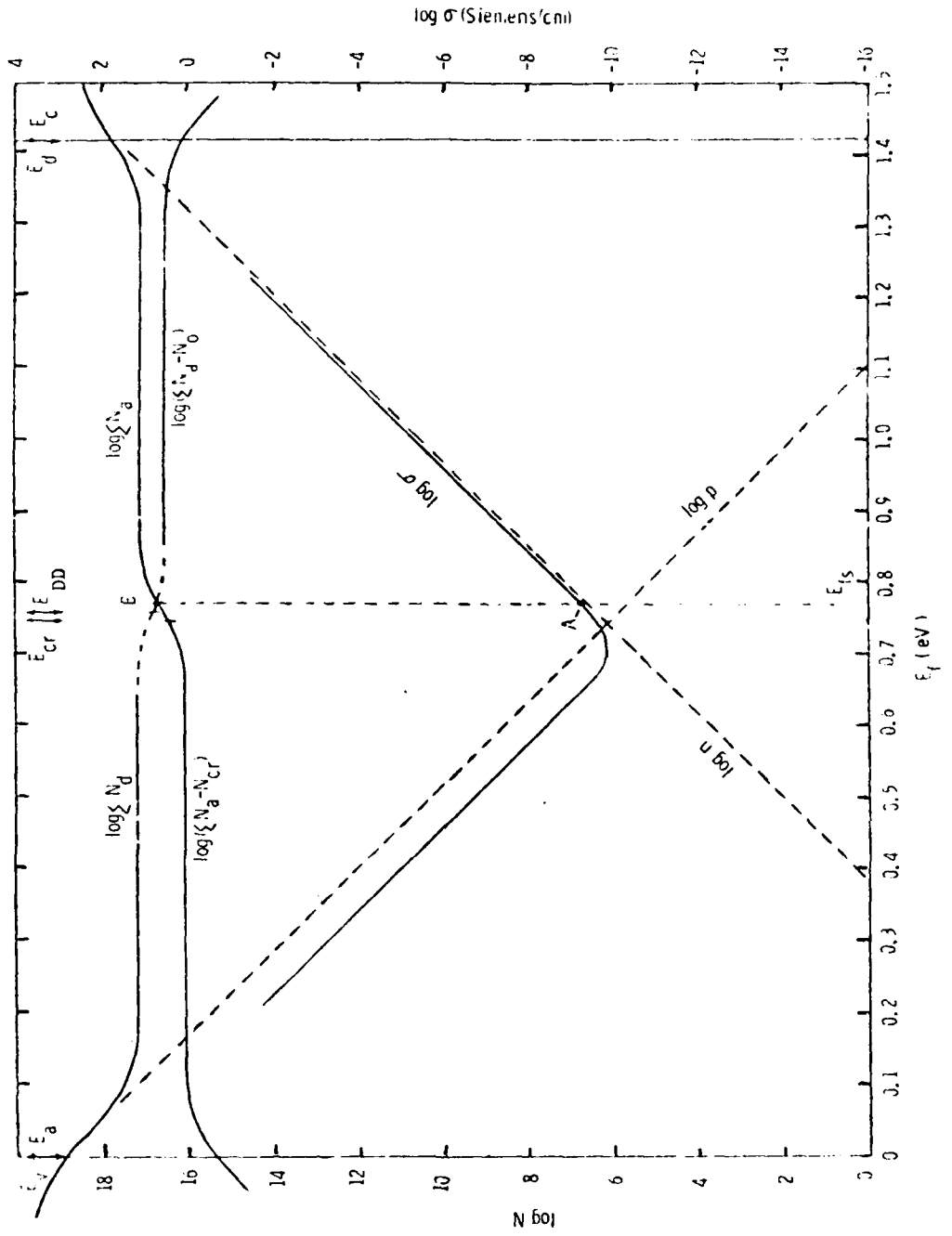

Figure 5. Determination of the energy of the oxygen level DD in GaAs from the experimental data of Reference 13. The energy levels of the shallow impurities are so close to those of the band edges that they are not distinguishable by separate double arrows. N represents n, p, $(\Sigma N_d^+ + p)$, $(\Sigma N_a^- + n)$.

chromium-free samples in the absence of another, deeper donor level. Recent studies (14) reveal the presence of just such a deeper donor level at about 0.76 eV that cannot be ascribed to oxygen. If we assume the upper extreme is correct for oxygen and that there is none of the mysterious deep donor at 0.76 eV (called EL-2 in the literature) present in sample L, then an oxygen concentration of 5×10^{16} atoms/cc. is necessary to produce the observed values of conductivity and Hall coefficient; a concentration only one third that detected by Lindquist. Indeed, it has been noted recently that spark source mass spectrograph measurements of oxygen concentration, such as those made by Lindquist, result in spuriously high values of oxygen due to excessive background. Helium temperatures spark source measurements (16) and SIMS (14) measurements made on a variety of GaAs specimens typically yield concentrations of 10^{16} or less - too little to produce the results of Lindquist's measurements for any reasonable value of E_O. Since there is no reason to doubt the values of the concentrations of the other elements present, the placement of the oxygen level at 0.84 and the postulation of an oxygen concentration of $<10^{16}$ would require the presence of EL-2 as well, to attain consistency with the experimental results. Precise values of all of the concentrations and energy levels could be used in conjunction with the nomographic method to help resolve these uncertainties, as well as the true values of the degeneracies g. As already stated, the exact choice of g is not important in many cases. For instance, if the values of g are both set at one instead of two and four, in the analysis of Lindquist's data, the resulting "oxygen" energy level is found to be at 0.78 eV instead of 0.76; a difference too small to be resolvable with the present uncertainties in the other parameters and experimental data. For the analysis in the remainder of the paper we shall choose our deep donor level to lie at 0.76 V and denote it by D.D. This is also the value formerly attributed to oxygen by Haisty et al (17).

ANALYSIS OF IN SITU COMPOUNDED SEMI-INSULATING GaAs

Samples #11 and #17 were identically prepared and processed except that sample #17 was deliberately doped with 10^{16} chromium atoms per cubic centimeter. Since chemical analysis of sample #11 revealed other acceptors to be present at concentrations of less than a few time 10^{15} atoms per cm^3, the first approximation is that 10^{16} atom/cm^3 represents the entire acceptor concentration*,†,‡. Accordingly, our first step is to draw an acceptor curve

*The in situ B_2O_3 encapsulated LEC compounding/Czochralski growth process eliminated all dependence on quartz and carbon components. See Reference 1

†Of the common impurities only boron and phosphorous were detected in a spark source analysis of #11. (D. Walters, Wright State Univ, Dayton, O.) Except for Cr content, #17 is expected to be of similar purity.

‡A SIMS analysis of similarly grown Rockwell material revealed correspondingly low impurity concentrations, (including that of silicon) which is attributed to the in situ synthesis technique. R. D. Fairman & J. R. Oliver "Growth and Characterization of the Semi-Insulating III-V Materials Conf, Nottingham, England, Apr 1980.

with a total concentration of 10^{16} and with a step at an energy of 0.75 eV, the assumed energy level of chromium. Again we construct a conductivity curve using the independently determined values of μ_n = 2140 cm^2/Volt-sec. See Figure 6a. The Fermi energy is then determined from this curve and the measured n type conductivity, 1.34 x 10^{-9} Siemens/cm. Thus, we know that the (+) curve must intersect the acceptor curve at point B, which is in the vicinity of the deep donor level at 0.76 eV. Since the deep donor must be present in chrome-free #11 to make it semi-insulating, we assume it to be present in #17 as well, as the two specimens have been presumed identical except for chromium content. Accordingly, a step corresponding to g = 2 is drawn at 0.76 eV so that it passes through point B; thus fixing the total donor level at 10^{16}. The latter value is now taken to be that for sample #11 as well, and is used to draw a nomograph for specimen #11 to determine ΣN_a from the measured conductivity in a similar manner, see Figure 6b. The addition of the acceptor concentration so determined to the 10^{16} chromium content for sample #17 yields a new total acceptor concentration for that sample of 1.4 x $10^{16} cm^{-3}$. This acceptor value is now used to draw another nomograph for sample #17, and so begins another analytical cycle. Thus, a self-consistent iterative procedure results in an estimate of total acceptor and donor concentrations of both samples from a knowledge of the deliberately incorporated chromium content of one of them. The convergence is fairly rapid, as more than three cycles produce no further discernable changes in concentration values. The concentrations thus determined are ΣN_a = 1.5 x 10^{16}, ΣN_d = 1.4 x 10^{16} for #17, and ΣN_a = 4.6 x 10^{15}, ΣN_d = 1.4 x 10^{16} for #11 after three cycles.

Sample #9

Since less pure Ga was used in the fabrication of Specimen #9, its impurity concentrations are likely to be greater; and therefore it cannot be analyzed iteratively in conjunction with Sample #17, as was Sample #11. We can, however, find the concentration ratio of total donor to total acceptor content as follows from Figure 7. As for our other samples, we know from the conductivity and Hall measurements that the intersection between the (+) and (-) curves must occur somewhere along line AB in Figure 7, i.e., at the Fermi energy. The only impurity levels in this region capable of producing steps in an impurity curve are the acceptors Fe and Cu, which are both at about 0.52 eV. This means that the plateau of the (+) curve must intersect the Fe-Cu step of the (-) curve on line AB. These requirements fix the ratio of total donor to total relevant acceptor concentration at 1.7. The qualifier, relevant, is used here because the acceptor plateau which intersects the donor curve represents the sum of ionized acceptors only. For reasonable concentrations the Cr level (if Cr is present) is too deep to influence the point of intersection. For this reason the quantity of interest here is $(\Sigma N_a - N_{Cr})/\Sigma N_d$ rather than the so-called compensation ratio $\Sigma N_a/\Sigma N_d$. Thus it is seen that useful information can be gleaned nomographically even in the absence of any quantitative knowledge of absolute concentrations. In the case of Sample #9, a knowledge of the value of conductivity and the sign of the Hall coefficient was sufficient for the deduction of the "compensation ratio," and the location of the energy level of the compensating acceptor together with its probable identity, namely Fe and/or Cu. The latter conclusion was subsequently confirmed by a chemical analysis which revealed iron to be the dominant impurity.

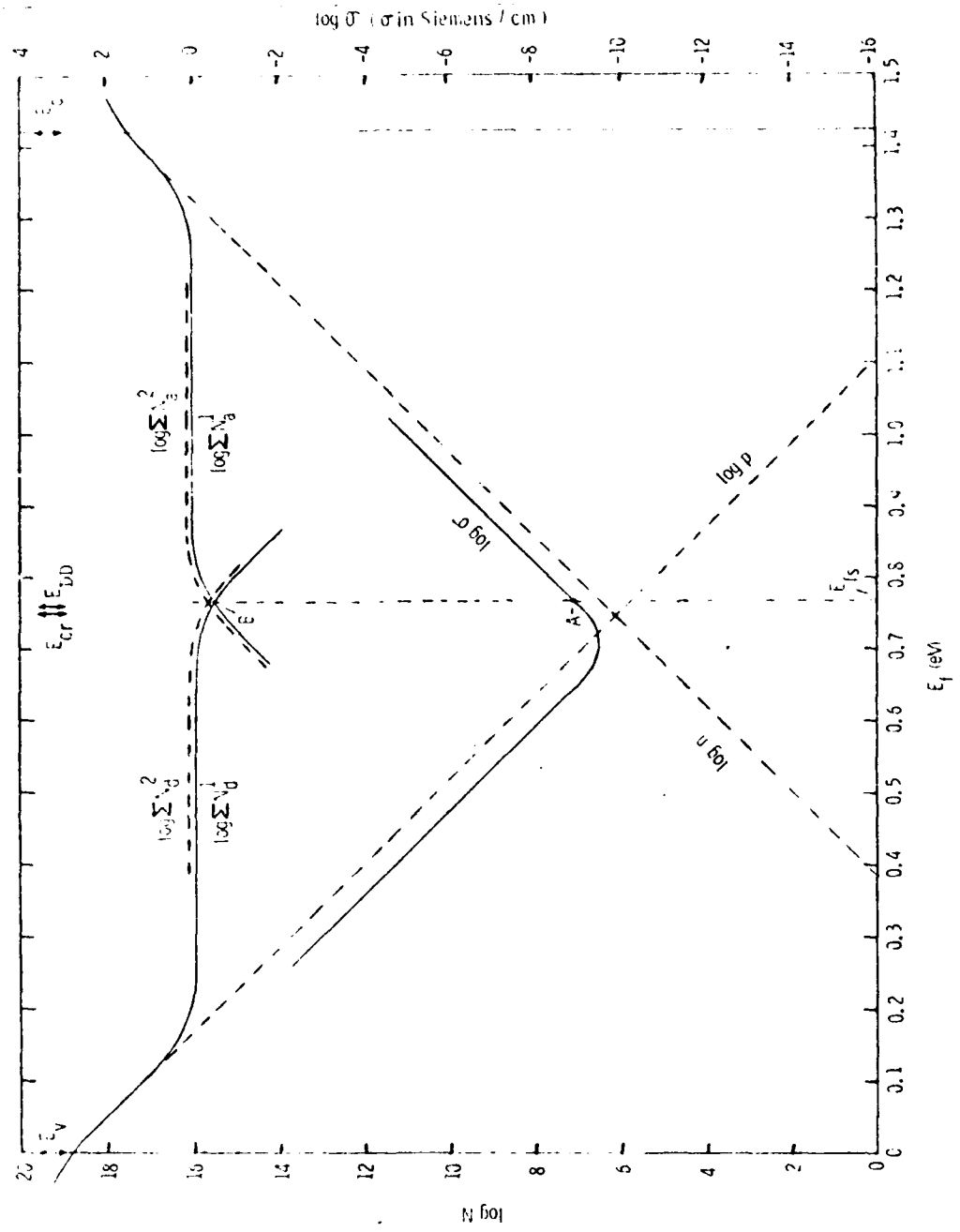

Figures 6a & 6b. Iterative determination of total donor and acceptor concentrations for sample #17 (Fig. 6a) and sample #11 (Fig. 6b). At the onset, ΣN_a^1 for #17 (Fig. 6a) is taken to be 10^{16} atoms/cm^3 which is the amount of Cr with which the sample was doped. From this, ΣN_d^1, the donor concentration is determined which is then taken to be the same as that for sample #11. From the latter, ΣN_a^1 for sample #11 is found in Figure 6b. This value is then added to the 10^{16} for sample #17 and the process is repeated with the new value ΣN_a^-. The second cycle is shown by the dotted curves in both figures. Subsequent cycles are not shown since they are so close to the second.

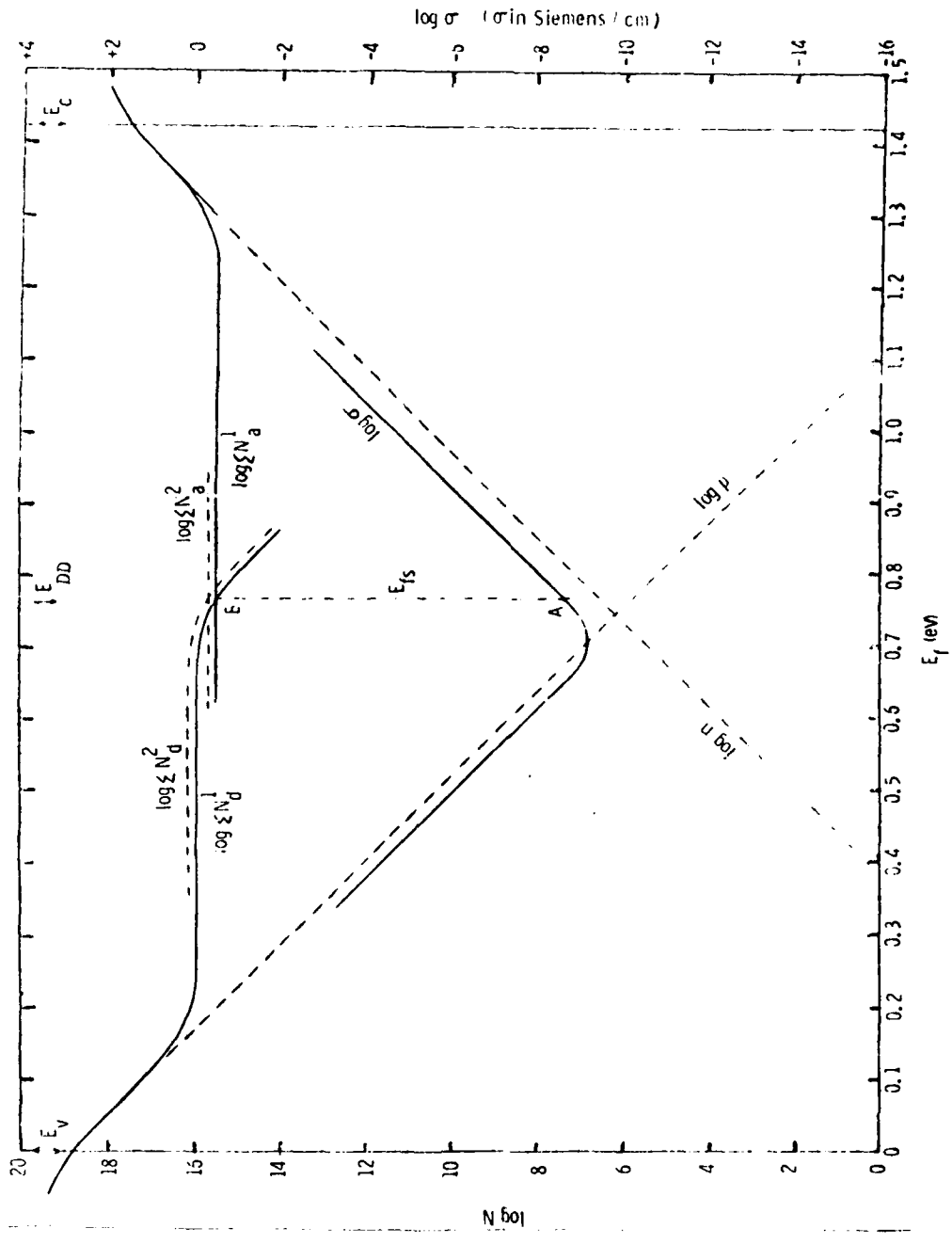

Figure 6b. Same as caption for Figure 6a.

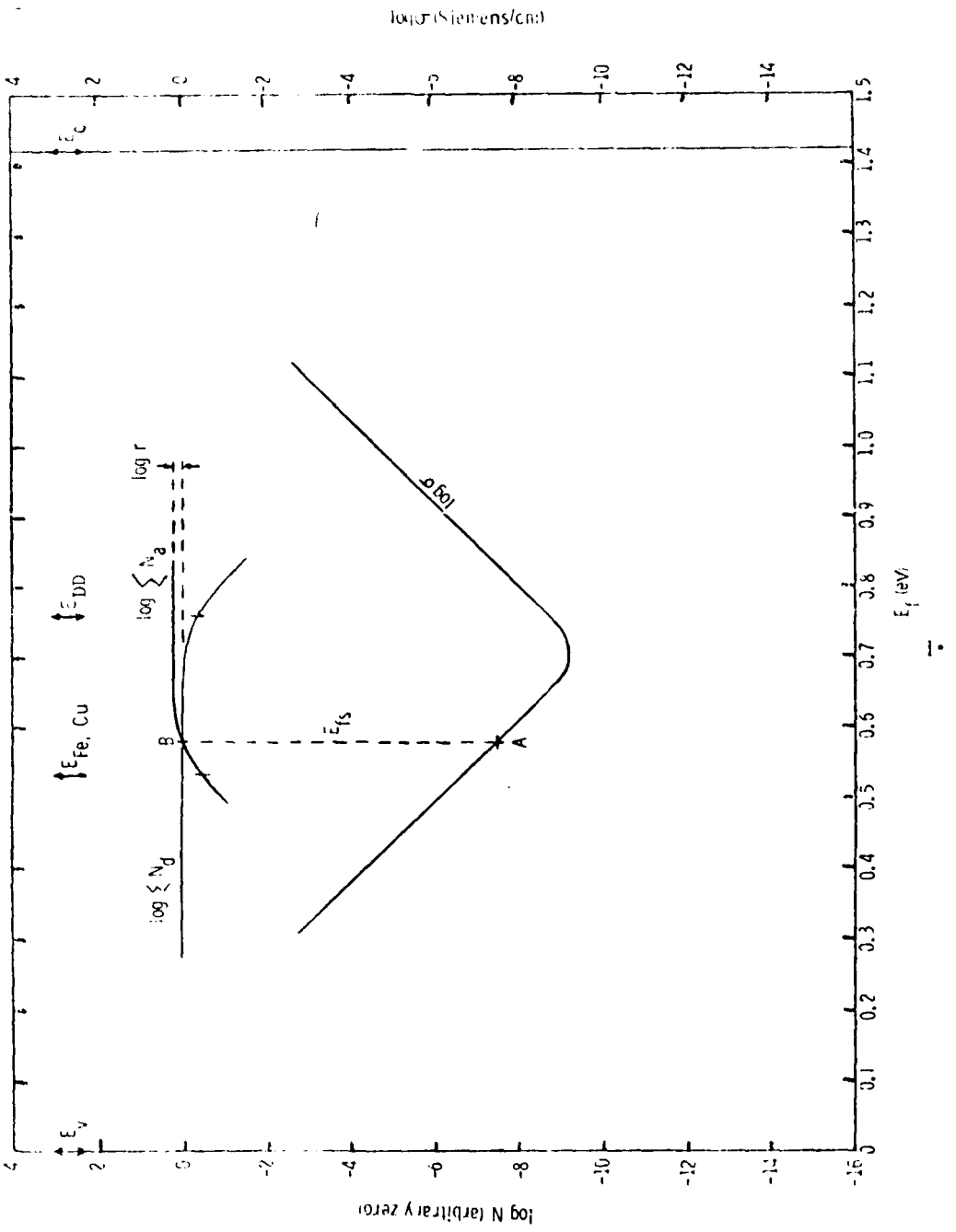

Figure 7. Detection of iron and/or copper in sample #9 and the determination of the compensation ratio $r = (\Sigma N_a - N_{Cr})/N_d$. The reason for the latter definition of r rather than the more familiar $r = N_a/N_d$ is that in this sample chromium plays no role in compensation.

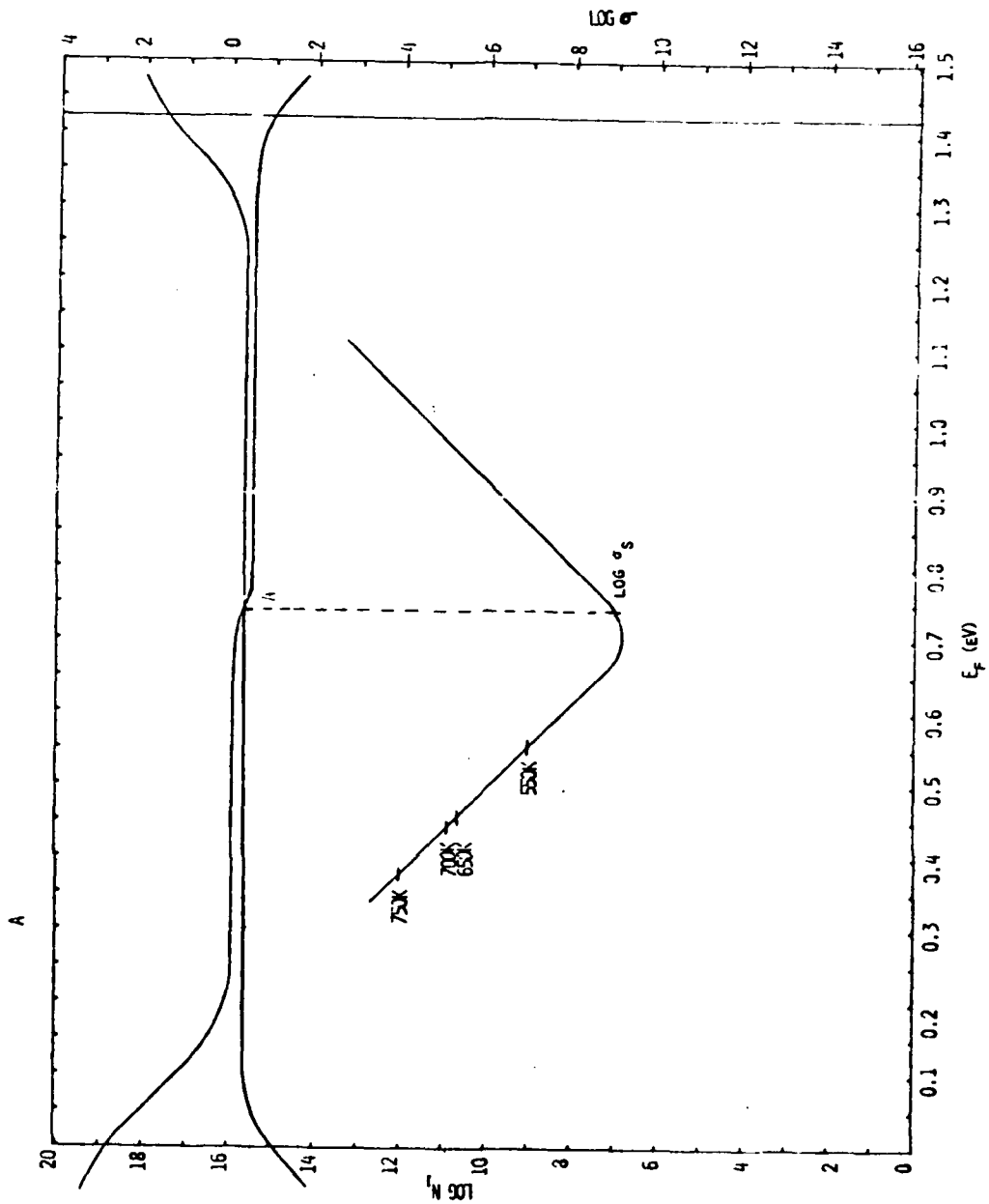

Figure 8a. Effect of heat treatment on a semi-insulating n-type GaAs specimen shows the sample state prior to heat treatment. Also shown are conductivities measured after each stage of the heat treatment.

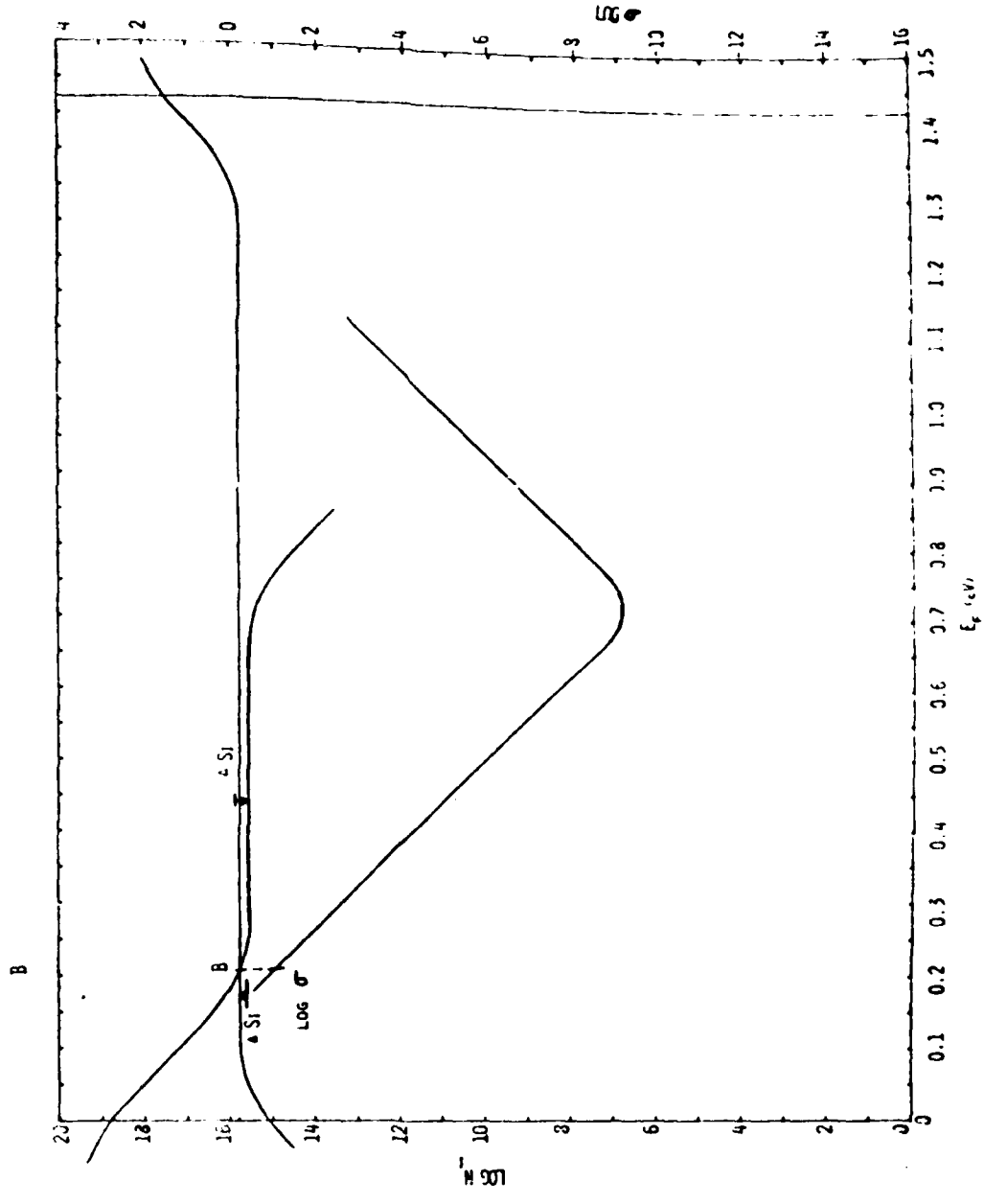

Figure 8b. Shows the effect of heat-induced conversion of Si from donor mode to acceptor mode on the total donor and acceptor concentrations. The arrows labeled $\mp \Delta S_i$ indicate the respective shifts in these concentrations.

APPARENT CONVERSION TO p-TYPE BEHAVIOR BY HEAT TREATMENT

When several semi-insulating samples of n type were heated for 30 minutes at each of successively higher temperatures, it was found that they would become p type and display steadily increasing conductivities with the completion of each temperature phase of the heat treatment. A simple tentative explanation for this behavior is suggested by a consideration of Figures 8a and 8b which show a nomograph for a typical semi-insulating chromium-free specimen of conductivity 10^{-9} Siemens/cm. Such specimens upon heat treatment will typically exhibit a sequence of increasing conductivities, such as those denoted in Figures 8a and 8b by the respective annealing temperatures applied to the sample prior to their determinations. Such a range of conductivities cannot be due to a bulk effect, since there are no impurity levels in the energy region (0.3 - 0.6 eV) which could bring about charge balance at the appropriate Fermi levels with the prevailing concentrations of known impurities. Further, etching the surfaces of the heat treated specimens gradually restores their original conductivities as successive surface layers are eaten away. Typically, the removal of surface to depth of about a micron is sufficient for complete restoration. Thus we conclude that the enhanced conductance resulting from the heat treatment occurs within a very thin surface layer in which the conductivity is enormously augmented.

One possible explanation is suggested by the observation that heating to the temperatures of the anneal results in an evaporation of arsenic and hence in an excess of empty arsenic sites near the surface*. Silicon impurity atoms then tend, under some conditions, to migrate to these empty sites from the Gallium sites where they are normally lodged, thus changing their status from shallow donors to shallow acceptors (19). This process results in a lowering of the total donor concentration and an accompanying raising of the total acceptor concentration. Figures 8a and 8b show the nomographs before and after anneal, respectively. The Fermi level moves leftward from A (Figure 8a) and, if the process continues so that ΣN_a becomes greater than ΣN_d, jumps abruptly to B (Figure 8b) with a concomitant rise in conductivity from 10^{-9} to about 0.1 Siemens/cm. The depth to which this alteration has occurred can be estimated for the various stages of anneal. We will consider the final state of the sample after it had been heated to 750 C. The mean sample conductivity at this stage was 10^{-4} Siemens/cm as shown in the figure. The conductance of a sample of square cross section of side a and length ℓ with a surface layer of depth δ is given by

$$G = \frac{4a\delta}{\ell}\sigma_s + \frac{(a-\delta)^2}{\ell}\sigma_b$$

*Another explanation is the diffusion of Mn from the bulk to the surface where it accrues to substantial concentrations 10^{17} cm^{-3} in a layer 1 to 3 microns thick (18). Thus, the Mn concentration becomes greater than the total donor concentration in the thin surface layer and again the intersection of the + and - curves moves to point B as in Figure 8b.

where σ_s and σ_b are the surface and bulk conductivities respectively. The mean conductivity σ_m is then

$$\sigma_m = G/a^2 = 4\frac{\delta}{a}\sigma_s + \frac{(a-\delta)^2}{a^2}\sigma_b$$

and since $a \gg \delta$

$$\sigma_m = \frac{4\sigma_s}{a} + \sigma_b$$

$$\delta = \frac{a(\sigma_m - \sigma_b)}{4\sigma_s} = \frac{a\sigma_m}{4\sigma_s}$$

since $\sigma_m \gg \sigma_b$ and $a = 0.2$ cm

$$\delta = \frac{0.2 \times 10^{-4}}{4 \times 10^{-1}} = 0.05 \times 10^{-3}\text{cm}$$

$$= 0.5 \text{ microns}$$

which is of the order of etching depths typically required to restore semi-insulating properties to GaAs samples which have been heat treated as described. It is possible that the migration of silicon atoms from gallium to arsenic sites may be supplemented by the loss of oxygen impurities at the sample surface which would, of course, also lower the total donor concentration to help bring it below the total acceptor concentrations.

In summary, conductivity and Hall measurements were used, together with a knowledge of the intrinsic parameters of GaAs, the energy levels of the relevant impurities, and the concentration of one dominant dopant (in this case Cr), to derive total donor and acceptor concentrations of two related samples. The ratio of ionized acceptors to total donors and the energy of the dominant acceptor (Fe) of another sample were determined without prior knowledge of the impurity content.

The effects of heat treatment on sample conductivity have been explained by a simple model with the aid of nomographs in a manner consistent with surface etching experiments. One can also set limits on the concentration of other impurities which may be present. Further, it has been demonstrated that besides furnishing a useful analytical tool, the nomographs provide a procedural guide for materials design and future experimentation. Perhaps most important of all, they enable one to depict in a single diagram all parameters germane to the conduction process, and clearly show exactly how any one of them would be affected by alteration of any of the others.

ACKNOWLEDGMENT

The authors would like to express their appreciation to Dave Look for corroborative measurements and useful discussions and to Roger Malik and Robert O. Savage for their assistance in preparing the samples.

LITERATURE CITED

1. T.T. AuCoin, R.L. Ross, M.J. Wade, R.O. Savage, "Liquid Encapsulated Compounding and Czochralski Growth of Semi-Insulating Gallium Arsenide," Solid State Technology 22, 59, (1979).

2. D.C. Look, "Mixed Conduction in Cr-Doped GaAs," J. Phys. Chem. Solids 36, 1311 (1975).

3. D.C. Look, "True Mobilities in Semi-Insulating O-and Cr-doped GaAs," Proceedings of the Semi-Insulating III-V Materials Conf, Nottingham, England, Apr 1980.

4. William Shockley, "Electron and Holes in Semiconductors," (D.Van Nostrand Co., New York, 1950) p.467.

5. Eberhard Spenke, "Electron Semiconductors," (McGraw-Hill Book Co, Inc, New York, 1958) p. 307.

6. R. Zucca, "Electrical Compensation in Semi-Insulating GaAs," J. Appl. Phys. 48, 198 (1977).

7. Patrick M. Hemenger, "Measurement of High Resistivity Semiconductor Using the Van der Pauw Method," Rev. Sci. Instrum. 44, 698 (1980).

8. S.M. Sze, "Physics of Semiconductor Devices," (Wiley - Interscience, New York, 1969) p. 57.

9. S.M. Sze and J.C. Irwin, "Resistivity, Mobility and Impurity Levels in GaAs, Ge, and Si at 300K," Solid State Electronics 11, 599 (1968).

10. E.H. Putley, "The Hall Effect and Related Phenomena," (Butterworths, London, 1960) p. 88.

11. D.C. Look, "The Electrical Characterization of Semi-Insulating GaAs: A Correlation with Mass Spectroscopic Analysis," J. Appl. Phys., 48 5141 (1977).

12. J. Betko and K. Merinsky, "Determination of the Electrical Properties of Semi-Insulating GaAs: A Role of the Magnetic Field Dependence of Single Carrier Parameters," J. Appl. Phys. 50, 4212 (1979).

13. P.F. Lindquist, "A Model Relating Electrical Properties and Impurity Concentrations in Semi-Insulating GaAs," J. Appl. Phys. 48 1262 (1977).

14. A.M. Huber and N.T. Link, "Direct Evidence for the Non-Assignment of Oxygen of the Main Electron Trap in Semi-Insulating GaAs," J. Appl. Phys., 48 1262 (1977).

15. B. Deveaud, P.N. Favennec, "Levels Obtained by Oxygen Implantation in Gallium Arsenide," Gallium Arsenide and Related Compounds 1978, St. Louis, Mo, USA 25-17, Sept 1978 (London, England: Inst. Physics 1979) pp. 492-500.

16. Dennis Walters, Wright State University, Dayton, Ohio. Private Comm.

17. R. W. Haisty, E.W. Mehal and R. Stratton, "Preparation and Characterization of High Resistivity GaAs," J. Phys. Chem. Solids 23, 829 (1962).

18. P.B. Klein, P.E.R. Nordquist and P.G. Siebenmann, "Thermal Conversion of GaAs," J. Appl. Phys. 51 4861 (Sept 1980).

19. W.Y. Lum and H.H. Wieder, "Photoluminescence of Thermally Treated n-type Si-doped GaAs," J. Appl. Phys. 49 6187 (1978).

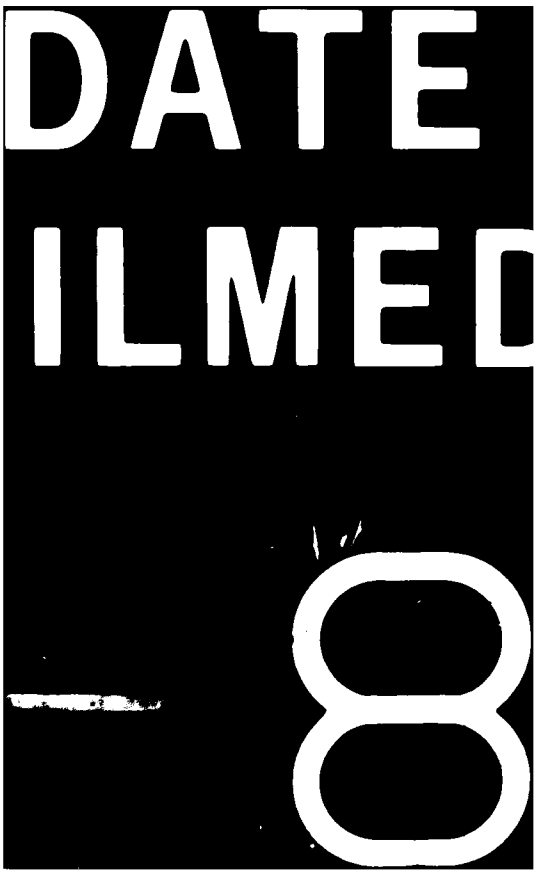
DATE
ILMED
8